PROCEEDINGS OF THE 15TH INTERNATIONAL CONFERENCE ON

OMAE

1996

OFFSHORE MECHANICS AND ARCTIC ENGINEERING

EDITED BY

S. CHAKRABARTI M. T. PONTES H. MAEDA J. FALZARANO
P. SCHOFIELD W. S. ATKINS D. MORRISON

VOLUME I – PART A
OFFSHORE TECHNOLOGY

PHYSICAL MODEL TESTS AND NUMERICAL SIMULATIONS OF A PIPELINE UNDER WAVE ACTION

J.L.J. Marchal, Ph. Rigo, Y. Pirenne, H. Wang
University of Liege , Liege
Belgium

Yucheng Li, Guozhang Lai, Ge Wang, Bin Chen
Dalian University of Technology , Dalian
China

ABSTRACT

The. results from two physical model tests of wave forces on a pipeline and a numerical simulation are given in this paper. The data from the two models with irregular waves are compared. It shows that within the test condition, ($0.5*10^4<Re<0.38*10^5$ and $3<KC<22$), when the scale between two models is 1:2, the scale effect coefficients of horizontal force are about 0.5 and 0.6 for e/D=0.0 and e/D=0.2 respectively. For the vertical force, they are about 0.8 and 0.89. The scaled model test will overestimate the wave forces. The results from numerical simulation of a regular wave have been compared with the test results and they correspond quite well.

1. INTRODUCTION

Pipelines are often used for offshore oil and gas developments and other offshore applications. The wave forces acting on a pipeline are the most important exciting forces, which depend on the flow behaviour around the pipeline. Since the flow behaviour is not well understood, the designers can not determine the wave forces accurately. Therefore, a model test is normally required. As well known, the forces acting on a pipeline by waves are mainly determined by two phenomena, i.e. velocity distribution and acceleration distribution of the wave flow, which are normally governed by Re and KC (see Eq.2). Physically, the viscous effect, namely surface friction, flow separation, wake and vortex, has great influence. In such cases, the Reynolds number is an important factor and the results from the scaled model on Froude Laws can not be directly used for the prototype. The purposes of this study are: firstly to run physical model tests in two different dimensions in order to know more about the flow behaviour and the scale effect; secondly to compare the numerical simulation with the model test in order to know the accuracy of the numerical simulation, which has the advantages in this area since there is no scale effect in numerical study. The numerical model was calibrated with the present experimental data. For the future, extended comparison with prototype measurements and for a wider range of Re and KC parameters is necessary in order to assess the model reliability. This is a joint research project between the University of Liege in Belgium and Dalian University of Technology in China. Two model tests were carried out separately, and the numerical simulation was conducted in Dalian University of Technology.

2. PHYSICAL MODEL TEST FACILITIES

2.1. Physical Model Test 1 (Model 1)

The definition sketch of a pipeline test is shown in Fig.1. The test was achieved to assess a new concept of immersed pipelines (Marchal and Rigo 1993). Model 1 was carried out in a wave flume, which was 17 m long, 1 m wide and 1.5 m high in the test section. The test cylinder (pipeline) with a diameter of 0.04 m was fixed through a load cell on the side wall of the wave flume (Aulanier et al, 1993). Irregular waves are mainly touched in model 1. For each water depth, d=0.165m, 0.231m or 0.298m, the significant wave height and the peak period of irregular waves, H_s and T_p, are varied within the limitations given in Tab.1. Two arrangements of the pipeline, e/D=0.0 and 0.2, had been studied. The surface elevation, horizontal and vertical force components were measured during the experiments.

2. 2 Physical Model Test 2 (Model 2)

The model test 2 (Model 2) was conducted in the wave-current flume in the State Laboratory of Coastal and Offshore Engineering, Dalian University of Technology. The flume is 69m long, 2m wide and 1.8m deep. The pipeline model (0.8m long, 0.08m in diameter) was connected with two-dimensional load cells at both ends, and the cells were fixed on two supporters. On the other side of the supporters, there were two individual dummy pipe models to mitigate the end effects. During the test, surface elevation, horizontal and vertical force components were measured, and both regular and irregular waves were studied. The test conditions are listed in Tab.2 and Tab.3.

3. DATA ANALYSIS OF THE MODEL TEST AND THE NUMERICAL SIMULATION METHOD.

3.1. Data Analysis of Regular Wave Forces

Regular waves are only concerned by model 2 and the LES numerical simulation (see hereinafter). The data are analysed by the following procedure:

3.1.1 Horizontal (or In-line) forces: The Morison Equation, Eq.(1), is used for in-line force analysis. The drag and inertia force coefficients, C_d and C_m, are determined by the Least Square Method (LSM)

$$f_x(z,t) = 0.5\rho C_d DU(z,t)|U(z,t)| + \rho C_m S\frac{\partial U(z,t)}{\partial t} \tag{1}$$

In Eq.(1), U(z,t) is the local undisturbed velocity which is calculated by the cnoïdal wave theory and steam function theory. U_{max} is defined as the amplitude of U(z,t). Then,

$$\mathrm{Re} = \frac{U_{\max}D}{\gamma}, \quad \text{and} \quad KC = \frac{U_{\max}T}{D}. \tag{2}$$

3.1.2 Lift forces: The maximum lift force coefficients are defined as follows:

$$C^{+}_{L\max} = f^{+}_{L\max} / 0.5\rho D U^2_{\max} \tag{3}$$

$$C^{-}_{L\max} = f^{-}_{L\max} / 0.5\rho D U^2_{\max} \tag{4}$$

where "+" means the vertical force acting upward, "-" means the vertical force acting downward.

3.1.3 Resultant forces: The resultant force is calculated as

$$f(t) = \sqrt{[f_x(t)]^2 + [f_l(t)]^2}$$

and the directional angle is

$$A_{f(t)} = \pm arctg[f_l(t) / f_x(t)]$$

The maximum resultant force coefficients are defined as:

$$C_{f\max} = f_{f\max} / 0.5\rho D U^2_{\max} \tag{5}$$

Assuming $A_{f\max}$ is the directional angle of the maximum resultant force.

3.2. Data Analysis of the Irregular Wave Forces

For irregular wave tests of the two models, force coefficients are also adopted to analyse the wave forces on a pipeline.

$$C_{fx} = \frac{(F_x)_{1/10}}{0.5\rho D U^2} \tag{6}$$

$$C_{fz} = \frac{(F_z)_{1/10}}{0.5\rho D U^2} \tag{7}$$

where U is calculated by two different approaches:

Analysis 1: U is defined as the amplitude of a significant local undisturbed velocity of irregular wave flow, which is calculated on the significant wave depth H_s and the peak period T_p by linear wave theory, i.e.

$$U = U_{\max} = \frac{\pi * H_s}{T_p}\frac{\cosh(k(e+D/2))}{\sinh(k*d)} \tag{8}$$

Analysis 2: Based on the JONSWAP spectrum $S(f_m)$ of irregular waves, for each frequency interval f_m, $H(f_m)$, $T(f_m)$ and $k(f_m)$ are calculated from H_s and T_p (Pirenne Y., 1995). Using the superposition principle, the local velocity u(t) is calculated by Eq.(9).

$$u(t) = \sum_{fm} \frac{\pi\ H(fm)}{T(fm)} \frac{\cosh\big(k(fm)*(e+D/2)\big)}{\sinh\big(k(fm)*d\big)} \cos\left(\frac{2\pi}{T(fm)}t + \phi_m\right) \tag{9}$$

in which the phase ϕ_m is a random variable.

The irregular wave free surface is divided into individual waves by the zero up-crossing method and the maximum velocity corresponding to each individual wave is calculated. Then the average of tenth highest velocities $U_{1/10}$ is used for the determination of the force coefficients (Eqs. 6 and 7).

For the first analysis, Re and KC are defined as those for regular wave analysis of Model 2 (see Eq.2); while for the second analysis $U_{1/10}$ and T_p are used.

Based on the research experience, Eq.(10) is supposed to give the best simulation of the relation between C_{fx}, C_{fz} and Re, KC.

$$C_f = \left(\frac{a}{\log\ \mathrm{Re}}\right)^b * KC^c \tag{10}$$

in which a, b and c are constants which are determined by regression analysis. Because the parameter e/D, also has a substantial influence on the flow behaviour around the pipeline, it is reasonable to divide the data from the two models into two groups, e/D=0.0 and e/D=0.2. Further tests for different values of e/D will be made in order to get more data and introduce e/D in the regression analysis (Eq. 10). Table 4 gives the regression results, which are also shown in Fig.2 for e/D=0.0. The relative errors of the regression results are also calculated. It seems that all the regression analysis are quite successful.

The analysis 2 provides also good regression results (with Eq. 10) with relative errors between 0.11 and 0.21.

3.4. Numerical Simulation:

There are mainly three ways to find a numerical solution of the Navier-Stokes Equation, which governs the problem. That is the direct numerical simulation (DNS), the $K-\varepsilon$ model and the large eddy simulation (LES). It has been proved that the LES method is more efficient and less artificial (Wang G., 1995). In the present study, the LES method is used, which can be written as follows

$$\frac{\partial u_i}{\partial t} + u_j\frac{\partial u_i}{\partial x_j} = -\frac{\partial p}{\partial x} + \frac{1}{\mathrm{Re}}\frac{\partial^2 u_i}{\partial x_j^2} + \frac{\partial}{\partial x_j}(\tau_{ij}) \tag{11}$$

$$\frac{\partial u_i}{\partial x_i} = 0 \tag{12}$$

where

$$\tau_{ij} = \gamma_s \left(\frac{\partial u_i}{\partial x_j} + \frac{\partial u_j}{\partial x_i}\right) \qquad (13)$$

$$\gamma_s = (C\Delta_{ij})\{2[(\frac{\partial u}{\partial x})^2 + (\frac{\partial v}{\partial y})^2] + (\frac{\partial u}{\partial y} + \frac{\partial v}{\partial x})^2\}^{1/2} \qquad (14)$$

C is the Smagorinsky constant, C=0.1 is adopted in this study. Δ_{ij} is the characteristic length of the calculated grid, here $\Delta_{ij} = \sqrt{S_{ij}}$, in which S_{ij} is the area of the calculated grid. In the analysis, $Re = u_m D / \gamma$, $KC = u_m T / D$, where U_m is the amplitude of the oscillating flow velocity. The free surface is not simulated at this stage, and oscillating flow with fixed boundary is adopted as the approaching flow condition.

4. RESULTS AND COMPARISON

4.1. Force Comparison between the Two Models

The geometric ratio of the test pipeline between model 1 and Model 2 is 1:2. For each group of the irregular wave test of Model 2 (see Tab.3), the corresponding hydraulic conditions in model 1 may be calculated by Froude Laws. Then, the forces from both models are listed in Tab.5 for e/D=0.0 and e/D=0.2, in which the forces from Model 1 are calculated based on the regression analysis.

According to Froude Laws, the force ratio, $(F_x)_2/(F_x)_1$ and $(F_z)_2/(F_z)_1$, between the two models should be 4.0. But Tab.5 shows that the ratio between the two horizontal forces is smaller than 4.0, while the ratio between the two vertical forces is close to the value by Froude Law. With exception of the difference of the two test facilities, this may be explained by the scale effect, or viscous effect. It means that for horizontal forces, the average viscous effect coefficients are approximately 0.6 to both e/D=0.0 and e/D=0.2. For the vertical forces, they are 0.9 and 0.8 when e/D=0.0 and e/D=0.2 respectively. This conclusion is only based on the comparison of several tests. More detailed discussion will follow.

4.2. Scale Effect Based on the Force Coefficients of the Two Models

Based on Re and KC, regression analysis (fig. 2) gives the force coefficient expressions as

for: e/D = 0.0 Re = 4928 to 38411 and KC = 3.43 to 22.64

$$C_{fx} = (\frac{5.7772}{\log Re})^{5.9306} * KC^{-0.1527} \qquad (15)$$

$$C_{fz} = (\frac{11.1858}{\log Re})^{1.9867} * KC^{-0.1761}$$

for: e/D = 0.2 Re = 5164 to 38437 and KC = 3.44 to 20.05

$$C_{fx} = (\frac{5.9296}{\log Re})^{4.7363} * KC^{-0.08199} \qquad (16)$$

$$C_{fz} = (\frac{24.4805}{\log Re})^{1.1519} * KC^{-0.3324}$$

Equations (15)-(16) confirm clearly the influence of Re and KC on the force coefficients. It shows that the force coefficient will decrease with both Re and KC increase. Within the limitation, $0.5*10^4 < Re < 0.38*10^5$ and $3 < KC < 22$, the scale effect on the force coefficient can be evaluated by those equations. The scale effect is defined as the ratio of the force coefficients between the two different scaled models. Table 6 gives the calculation when the model scale is 1:2.

In practice, even if it is well known that the wave forces are strongly influenced by the Reynolds number, it is not unusual to use Froude model. Such Froude models are, for instance, used when immersed piping system with new features must be assessed (Marchal et al., 1993). According to Froude Laws, the force coefficient and the KC number will not change with the model scale. The scale effect is, then, clearly a matter of Re number.

From Tab.6, one can see that when the model scale is 1:2, the scale effect coefficients on horizontal forces are about 0.5 and 0.6 for e/D=0.0 and e/d=0.2 respectively. For vertical force, they are 0.8 and 0.89. In the previous paragraph, the scale effect coefficients have been discussed through several direct comparisons. Because the calculations of Tab.6 are based on all of the available tests of the two models, it seems that the conclusion here is more reliable, and it is valid to $0.5*10^4 < Re < 0.38*10^5$ and $3 < KC < 22$.

The similar conclusions can be made from the results given by the analysis 2 (Eq. 9). When the model scale is 1:2, the horizontal scale effects are 0.56 and 0.60 for e/D=0.0 and e/D=0.2 respectively and for the vertical forces, they are 0.89 and 0.80.

Since the results of both analysis correspond quite well with each other, the first approach , whose handling is easier, based on the linear theory for a free stream flow is recommended for the force coefficients (Eqs.15-16) and the scale effect calculations.

In an other study, Jacobsen (et al, 1984) consider the flow disturbances caused by the presence of the pipe on the seabed. If the velocity is measured at a location above and close to the pipe, Jacobsen shows that the calculation of the force coefficients gives almost constant values for a wide range of KC, which is rather different than the free stream method (Sarpkaya et al, 1981).

4.3. Comparison between Physical Model Test and Numerical Simulation

For the regular wave study, comparisons between the model test results and the numerical simulations are shown in Tab.7, Tab.8 and Figs.3, Fig.4 and Fig.5. Figure 3 gives the comparison of the surface profile. The computation is based on the cnoïdal wave theory and steam function theory. Figure 4 and Figure 5 give the comparisons of the force measurements and LES results only for the test R33E0. Other tests are also simulated with the similar tendency.

From Tab.7 and Tab.8, one can see that the drag force coefficients, C_d, the upward lift force coefficients, $C_{lmax}(+)$, and the maximum resultant force coefficients, C_{fmax}, from LES are very close to those from the model test. But the inertia force coefficients, C_m, from LES are much greater than those from physical testing. As mentioned in the following paragraph, the in-line forces from LES, which are the combination of the drag forces and the inertia forces, are very close to the measured data. It means that in this study, it is in a drag dominant condition. Therefore, the discrepancy of initial force coefficients between the numerical simulation and physical test will not cause big problems for the final results, namely the in-line forces. The downward lift force coefficients, $C_{lmax}(-)$, and the directional angle of the maximum resultant forces, A_{fmax}, from LES are a little larger than those from the model test.

Figure 3 shows that the calculated wave surface profile, which is based on the cnoïdal wave theory and steam function theory, agrees well with the experimental data, which proves that the velocity calculation in the test data analysis is credible.

Figure 4 gives an example of the comparison of the in-line and vertical forces between the model test and LES. They correspond quite well with each other, except for a small phase shrift. And the vertical forces are not so well simulated as in-line forces. Note that the in-line forces are considered as two parts, i.e. the drag force and the inertia force, and the inertia force coefficient is not well simulated, as mentioned in the previous paragraph. It means that, in this study, the drag force is a dominant component.

Figure 5 shows that the calculated resultant forces and the directional angle of the calculated resultant forces correspond quite well to the measured test data, but there is also a small phase shift between them.

A more comprehensive paper concerning the comparison of the LES method and various experimental datas will be published further. The presented comparison is only valid for a limited range of the KC and Re numbers. The validation of the LES model to an other range of these parameters is now considered in order to apply the numerical model to practical application and design.

5. CONCLUSIONS AND REMARKS

1. In the analysis of irregular wave forces, the velocity used in the local parameters, Re and KC, is calculated by linear wave theory from the significant wave height, H_s, and the peak period, T_p. Regression results show that the force coefficients are closely related with Re, KC and e/D. Since there are not enough data available, e/D is not included in the regression equation in this paper.

2. Two physical tests (on irregular waves) confirm that, because of the influence of the viscous effect, the wave forces acting on pipelines would not exactly follow the Froude Laws. Nevertheless, it is observed that model test based on the Froude law is often adopted for practical applications. Therefore a better understanding on scale effect means that more reliable design may be achieved. Within the test limitation, $0.5*10^4 < Re < 0.38*10^5$ and $3 < KC < 22$, if the scale between two models is 1:2, the average scale effect coefficients on horizontal forces are about 0.5 and 0.6 for e/D=0.0 and e/D=0.2 respectively. For the vertical forces, they are 0.8 and 0.89. The scaled model tests will overestimate the wave forces.

3. By means of Large Eddy Simulation, the numerical solution of the flow behaviour around a pipeline is successfully developed. The results given by numerical simulation are quite close to those given by the model test (regular wave in Model 2). It means that the LES method is powerful for the calculation of pipeline problems. The future combined study will focus on the simulation of prototype pipelines.

REFERENCES

Aulanier, J.P., Naciri, M. and Staiquily, N., 1993, "Assainissement du Grand Casablanca Emissaire Sous-Marin D'el Hank" (in French), Bouygues Travaux Maritimes, France.

Chen, B., 1995, "Model Tests and Numerical Simulations of Waves Acting on Pipeline near the Sea Bottom ", M.S Dissertation, Dalian University of Technology, Dalian, P.R China.

Jacobsen, V., Bryndum, M.B., and Fredsoe, J., 1984, "Determination of Flow Kinematics Close to Marine Pipelines and Their Use in Stability Calculations", Proceedings, 16th Annual Offshore Technology Conference, Houston.

Li, Y.C., 1989, " Wave Action on Maritime Structures", The Press of Dalian University of Technology, Dalian, P.R China.

Marchal, J.L.J., 1991, "Statics and Dynamics of Maritime Structures", Lecture Notes, University of Liège - ANAST, Belgium.

Marchal, J.L.J. and Rigo, Ph., 1993, "Stabilisation Test of the Casablanca Pipeline" (in French), LHCN, University of Liège, Belgium.

Pirenne, Y., 1995, " Stability of a Submerged Pipeline under Regular and Irregular Waves" (in French), M.S Dissertation, University of Liège, Belgium.

Sarpkaya, T. and Isaacson, M., 1981, "Mechanics of Wave Forces on Offshore Structures", Van Nostrand Reinhold Company.

Verley, R.L.P., Lambrakos, K.F., and Reed, K., 1987, "Prediction of Hydrodynamic Forces on Seabed Pipelines", Proceedings, 19th Annual Offshore Technology Conference, Houston. (See also OTC 5501, Wolfram et al., 1987; OTC 5502, Holthe et al., 1987; OTC 5503, Verley et al., 1987; OTC 5507, Lambrakos et al., 1987; OTC 5369, Fyfe et al., 1987).

Wang, G., 1995, "Numerical Study of a Circular Cylinder in 2D Oscillatory Flow Field", Ph.D. Dissertation, Dalian University of Technology, Dalian,P.R China.

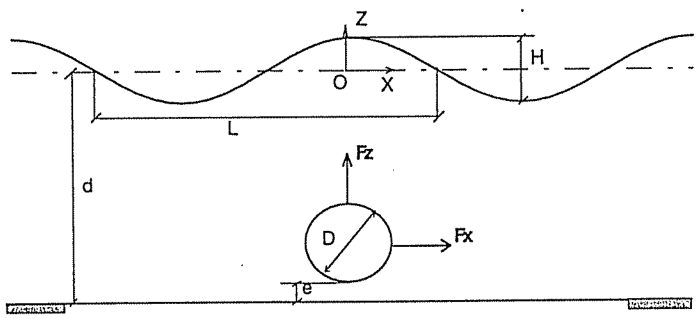

Fig.1 Definition Sketch of Pipeline Test

Tab.1 Test Conditions of Model 1

d(m)	e/D=0.0			e/D=0.2		
	H_s(m) (Max / Min)	T_p(m) (Max / -Min)	Number of tests	H_s(m) (Max / Min)	T_p(m) (Max / Min)	Number of tests
0.165	0.038 / 0.071	1.07 / 2.22	14	0.038 / 0.069	1.07 / 2.16	13
0.231	0.041 / 0.106	1.35 / 2.13	28	0.069 / 0.112	1.59 / 2.07	13
0.298	0.074 / -0.147	1.59 / 2.16	14	0.078 / 0.149	1.59 / 2.16	13

Tab.2 Regular Wave Tests of Model 2

d(m)	e/D=0.0			e/D=0.2		
	H(m)	T(s)	Code	H(m)	T(s)	Code
0.333	0.126	2.19	(R31E0)	0.129	2.19	(R31E2)
0.333	0.133	2.92	(R32E0)	0.134	2.92	(R32E2)
0.467	0.179	2.19	(R33E0)	0.188	2.19	(R33E2)
0.600	0.189	2.19	(R35E0)	0.199	2.19	(R35E2)
0.600	0.253	2.92	(R36E0)	0.276	2.92	(R36E2)

Tab.3 Irregular Wave Tests of Model 2

d(m)	e/D=0.0			e/D=0.2		
	H_s(m)	T_p(s)	Code	H_s(m)	T_p(s)	Code
0.333	0.131	2.19	(J31E0)	0.136	2.19	(J31E2)
0.333	0.130	2.92	(J32E0)	0.134	2.92	(J32E2)
0.467	0.193	2.19	(J33E0)	0.200	2.19	(J33E2)
0.467	0.193	2.92	(J34E0)	0.203	2.92	(J34E2)
0.600	0.188	2.19	(J35E0)	0.200	2.19	(J35E2)
0.600	0.253	2.92	(J36E0)	0.262	2.92	(J36E2)

Tab.4 Regression Results of the Force Coefficients in Two Model Tests

	C_f	$C_f=(a/\log Re)^b * KC^c$				Re	KC
		a	b	c	r	Max / Min	Max / Min
e/D=0.0	C_{fx}	5.7772	5.9306	-0.1527	0.130	38411 / 4928	22.65 / 3.43
	C_{fz}	11.1858	1.9867	-0.1761	0.206	38411 / 4928	22.65 / 3.43
e/D=0.2	C_{fx}	5.9296	4.7363	-0.08199	0.102	38437 / 5164	20.05 / 3.44
	C_{fz}	24.4805	1.1519	-0.3324	0.124	38437 / 5164	20.05 / 3.44

where 94 tests are included for e/D=0.0, while 43 tests are included for e/D=0.2.

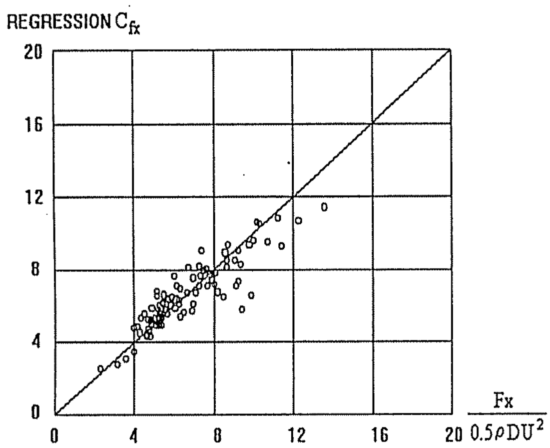

Regression Equation: $C_{fx}=(\frac{a}{\log Re})^b * KC^c$

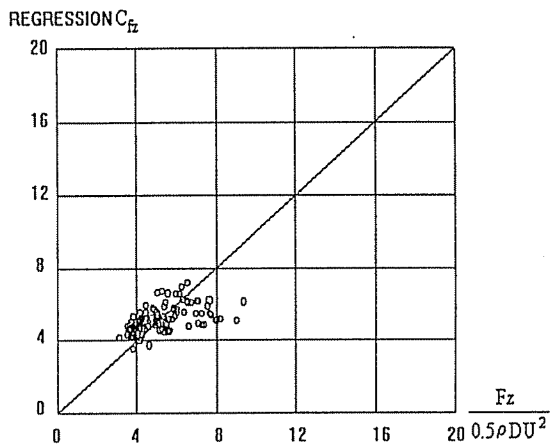

Regression Equation: $C_{fz}=(\frac{a}{\log Re})^b * KC^c$

Fig.2 Comparison of Regression and Test Force Coefficients (e/D=0.0)

Tab.5 Comparison of the forces between the two models

Code.	F_x (e/D=0)			F_z (e/D=0)			Code.	F_x (e/D=0.2)		F_z (e/D=0.2)		
	$(F_x)_2$ Model 2 (N/m)	$(F_x)_1$ Model 1 (N/m)	$(F_x)_2/(F_x)_1$	$(F_z)_2$ Model 2 (N/m)	$(F_z)_1$ Model 1 (N/m)	$(F_z)_2/(F_z)_1$		$(F_x)_2$ Model 2 (N/m)	$(F_x)_2/(F_x)_1$	$(F_z)_2$ Model 2 (N/m)	$(F_z)_1$ Model 1 (N/m)	$(F_z)_2/(F_z)_1$
J31E0	19.6	7.02	2.79	17.8	7.10	2.51	J31E2	14.4	2.24	10.0	4.90	2.04
J32E0	20.9	7.12	2.97	23.1	7.81	2.96	J32E2	14.9	2.20	13.2	4.78	2.76
J33E0	22.2	8.17	2.72	25.7	6.92	3.71	J33E2	19.8	2.62	18.2	5.61	3.24
J34E0	22.4	9.22	2.43	32.8	8.71	3.77	J34E2	21.1	2.27	19.4	6.49	2.99
J35E0	17.4	5.50	3.16	18.6	4.25	4.38	J35E2	14.7	2.85	16.9	3.70	4.57
J36E0	21.2	10.49	2.02	34.7	8.28	4.19	J36E2	24.2	2.45	22.3	6.43	3.47
		average	2.68		average	3.59		average	2.44		average	3.18

Tab.6 Scale Effect on Wave Forces with Scale 1:2

	KC	Model 1			Model 2			Scale Effect	
		Re_1	C_{fx1}	C_{fz1}	Re_2	C_{fx2}	C_{fz2}	C_{fx2}/C_{fx1}	$C_{fz2}/Cfz1$
e/D=0.0	3.43	4928	11.78	7.28	13938	5.94	5.79	0.50	0.79
		13580	6.04	5.82	38411	3.26	4.74	0.54	0.81
	22.65	4928	8.83	5.22	13938	4.45	4.15	0.50	0.80
		13580	4.53	4.17	38411	2.45	3.40	0.54	0.81
	Average							**0.52**	**0.80**
e/D=0.2	3.44	5164	8.30	5.82	14606	4.82	5.10	0.58	0.88
		13590	4.99	5.15	38437	3.06	4.57	0.61	0.89
	20.5	5164	7.17	3.22	14606	4.16	2.82	0.58	0.88
		13590	4.31	2.84	38437	2.64	2.53	0.61	0.89
	Average							**0.60**	**0.89**

Tab.7 Comparison of Regular Wave between Model 2 and LES

Code	Re	KC	C_d		C_m	
			Model 2	LES	Model 2	LES
(R31E0)	25735	8.85	3.94	4.06	1.24	4.19
(R32E0)	31959	14.65	3.11	3.45	0.67	2.14
(R33E0)	32099	11.03	3.99	3.99	0.79	5.41
(R35E0)	24348	8.37	3.84	3.70	0.88	3.78
(R36E0)	44535	20.41	1.80	2.70	0.26	2.39
(R31E2)	26026	8.95	3.54	3.53	0.69	2.91
(R32E2)	33191	15.41	2.17	4.34	0.39	2.49
(R33E2)	33984	11.68	3.40	4.37	0.38	3.59
(R35E2)	25732	8.85	3.32	2.96	1.06	2.38
(R36E2)	46955	22.09	1.72	2.41	0.23	1.48

Tab.8 Comparison of Regular Wave between Model 2 and LES

Code	C_{lmax} (+)		C_{lmax} (-)		C_{fmax}		A_{fmax}	
	Model 2	LES	Model 2	LES	Model 2	LES	Model 2	LES
(R31E0)	3.56	3.26	0.07	0.43	4.93	4.86	27.68°	47.22°
(R32E0)	3.19	4.41	0.27	0.02	3.67	5.50	46.83°	56.41°
(R33E0)	3.63	4.24	0.16	0.37	5.86	5.84	52.72°	56.79°
(R35E0)	3.38	3.41	0.03	0.35	3.95	4.45	42.53°	51.10°
(R36E0)	2.87	3.57	0.21	0.09	3.54	4.08	65.30°	61.08°
(R31E2)	2.61	2.22	2.11	1.69	3.57	3.83	27.29°	36.73°
(R32E2)	1.21	2.82	0.96	1.35	2.58	5.28	23.58°	25.31°
(R33E2)	2.03	2.30	1.09	1.19	4.64	4.53	39.38°	44.68°
(R35E2)	3.13	2.73	2.01	1.45	3.91	3.49	27.26°	35.79°
(R36E2)	1.70	1.33	0.38	0.27	2.31	2.80	39.81°	32.78°

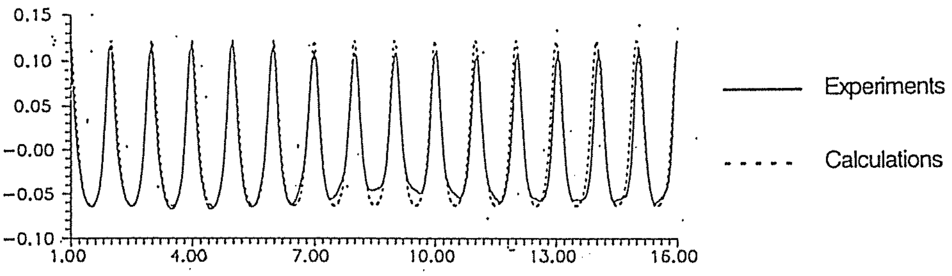

Fig.3 Comparison of Wave Surface Profile(R33E0)

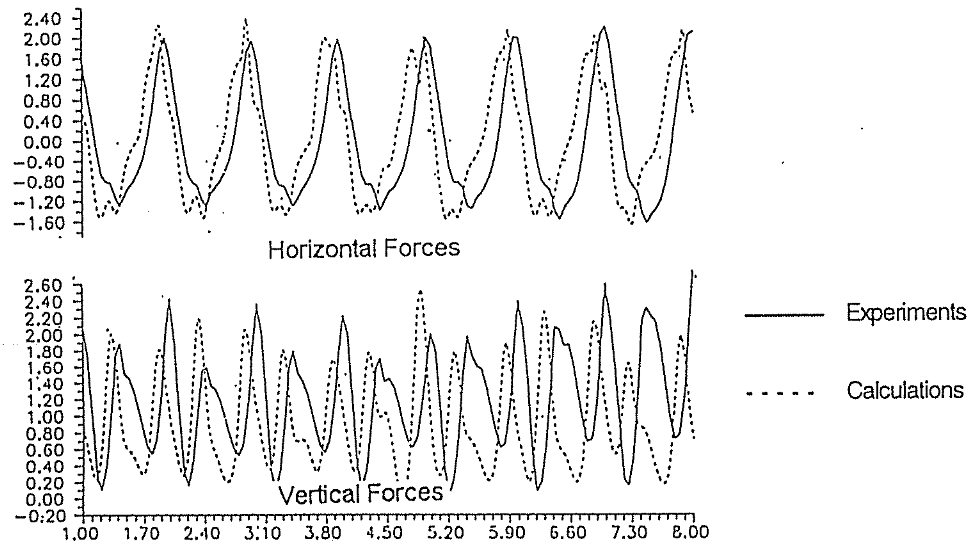

Fig.4 Comparison of Horizontal and Vertical Forces (R33E0)

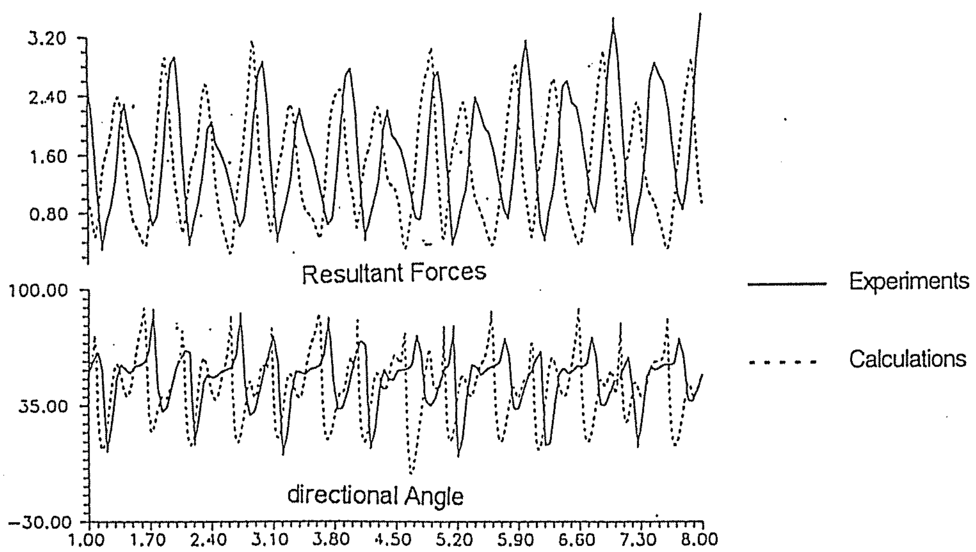

Fig.5 Comparison of Resultant Forces and Directional Angle (R33E0)